

# MgII Absorption through Intermediate Redshift Galaxies

Christopher W. Churchill<sup>1</sup>, Glenn G. Kacprzak<sup>1</sup>  
 and Charles C. Steidel<sup>2</sup>

<sup>1</sup>Department of Astronomy, New Mexico State University,  
 Las Cruces, NM 88003, USA  
 email: cwc@nmsu.edu, glennk@nmsu.edu

<sup>2</sup>Department of Astronomy, California Institute of Technology,  
 Pasadena, CA 91125, USA  
 email: ccs@astro.caltech.edu

## Abstract.

The current status and remaining questions of MgII absorbers are reviewed with an eye toward new results incorporating high quality *Hubble Space Telescope* images of the absorbing galaxies. In the end, we find that our current picture of extended gaseous regions around galaxies at earlier epochs is in need of some revision; MgII absorbing “halos” appear to be patchier and their geometry less regular than previously inferred. We also find that the so-called “weak” MgII absorbers are associated with normal galaxies over a wide range of impact parameters, suggesting that this class of absorber does not strictly select low surface brightness, dwarf galaxies, or IGM material. We emphasize the need for a complete survey of the galaxies in quasar fields, and the importance of obtaining rotation curves of confirmed absorbing galaxies.

**Keywords.** quasars: absorption lines; (galaxies:) absorption lines; galaxies: evolution, formation, structure, ISM, halos

## 1. Introduction

Studying MgII absorption lines holds the promise of placing powerful constraints on scenarios of galactic formation and evolution. MgII absorption is arguably the best tracer of metal-enriched gas *associated with galaxies*. Magnesium is an  $\alpha$ -process element ejected by supernovae into interstellar, intergroup, and intergalactic space from the time of the very first generation of stars to the present epoch. Furthermore, MgII absorption arises in gas spanning more than five decades of neutral hydrogen column density, from  $\log N(\text{HI}) \simeq 15.5$  to greater than 20.5 [atoms  $\text{cm}^{-2}$ ] (e.g., Bergeron & Stasińska 1986; Steidel & Sargent 1992; Churchill *et al.* 2000a); it therefore probes a wide range of HI environments associated with star formation, i.e., galaxies.

MgII systems are observed in the optical over the large redshift range  $0.3 \leq z \leq 2.2$ , are common (about one for every unit of redshift), and are easily identified in quasar spectra. Shown in Figure 1 (upper panel) is an example of a typical MgII system and its associated MgI and FeII absorption. The tall-tale signature of these systems is unambiguous. In order to exploit these systems for studies of galaxy evolution, it is imperative to establish the connections between the absorbing gas properties and the galaxy properties.

The kinematics of MgII absorbers loosely correspond to the type of galaxy environment and HI column density regime being probed. In Figure 1 (lower panels), three “classes” of absorber kinematics are presented. These classes are more generally based upon a multivariate statistical analysis incorporating associated high ionization and HI absorption properties (Churchill *et al.* 2000b).

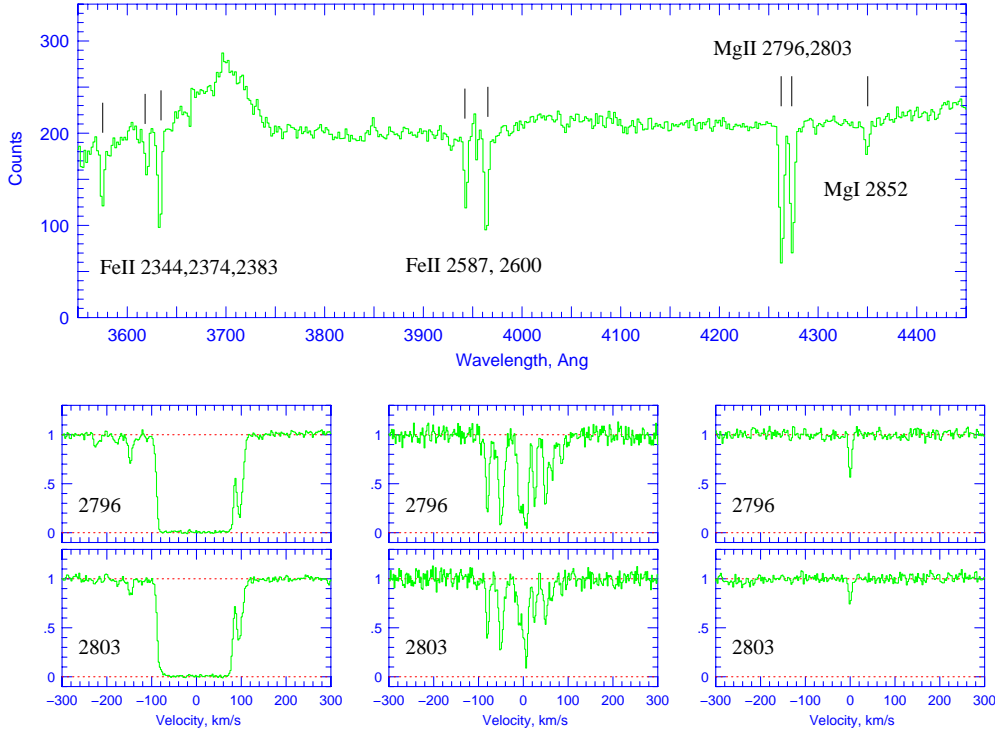


**Figure 1.** — (upper) A typical strong MgII absorber at a resolution of  $1.5 \text{ \AA}$  showing the MgII doublet and accompanying MgI and FeII absorption (from the survey of Steidel & Sargent 1992). — (lower) The kinematic “morphology” of three classes of MgII absorbers, (left) DLA/HI-rich, (center) LLS/classic, and (right) weak system (from the survey of Churchill & Vogt 2001).

**DLA/HI-Rich Systems** (lower left panel): When the MgII profiles are fully saturated with no discernible velocity substructure, the system is often a damped Ly  $\alpha$  absorber (DLA) with  $\log N(\text{HI}) \geq 20.3 \text{ cm}^{-2}$ . The MgII kinematics range between  $100\text{--}200 \text{ km s}^{-1}$  and are rarely seen to have “kinematic subsystems” (higher velocity absorption). The associated galaxies are observed to be a “mixed-bag” of morphologies and luminosities, including low surface brightness galaxies (Bowen, Tripp, & Jenkins 2001) and sub- $L^*$  to  $L^*$  galaxies (Le Brun *et al.* 1997; Rao *et al.* 2003; also see Figure 5).

**Classic Systems** (lower center panel): When the MgII profiles exhibit a complex run of optical depth with velocity, the system is often a Lyman limit system (LLS) with  $\log N(\text{HI}) \geq 17.3 \text{ cm}^{-2}$ . The MgII kinematics range between  $50\text{--}400 \text{ km s}^{-1}$  and often have higher velocity weak, narrow, kinematic subsystems. The kinematics can vary greatly from system to system and it is difficult to identify a “poster-child” example. The associated galaxies are often fairly normal appearing, bright, spiral galaxies (Steidel *et al.* 1998; also see Figure 5).

**Weak Systems** (lower right panel): At very low equivalent width,  $W_r \simeq 0.1 \text{ \AA}$ , the MgII profiles are often unresolved in high resolution spectra. The system is often a sub-LLS absorber with  $\log N(\text{HI}) \leq 16.8 \text{ cm}^{-2}$ . Some weak absorbers have multiple “clouds” spread over  $10\text{--}100 \text{ km s}^{-1}$ , but most are single clouds. It has been suggested that these systems are associated with low surface brightness galaxies (Churchill & Le Brun 1997), intergalactic star forming “pockets” (Rigby *et al.* 2002) or dwarf galaxies (Zonak *et al.* 2004).

## 2. MgII Absorbers: A Brief Overview

There is a rich history of the study of MgII absorbers that cannot be given full justice in this short paper. However, a non-exhaustive survey of the literature provides a reasonable representation of the variety of excellent contributions over the last decade and a half. In Table 1, a brief list of MgII absorber related literature is presented by three categories: spectroscopic surveys, studies of the galaxy properties, and modeling of galaxy halos and ionization conditions.

**Table 1.** Non-Exhaustive MgII Absorber Literature

Spectroscopic	Galaxy Connection	Modeling
<b><u>UV Surveys</u></b>	<b><u>Surveys</u></b>	<b><u>Galaxy Halos</u></b>
Churchill <i>et al.</i> (2000a)	Yanny (1990)	Gruenwald & Viegas (1993)
Churchill (2001)	Lanzetta & Bowen (1990)	Srianand & Khare (1993)
<b><u>Optical Surveys</u></b>	Bergeron & Boissé (1991)	Phillips <i>et al.</i> (1993)
Lanzetta <i>et al.</i> (1987)	Bechtold & Ellingson (1992)	Mo & Miralda-Escudé (1996)
Tytler <i>et al.</i> (1987)	Le Brun <i>et al.</i> (1993)	Charlton & Churchill (1996)
Sargent <i>et al.</i> (1988b)	Drinkwater <i>et al.</i> (1993)	Charlton & Churchill (1998)
Caulet (1989)	Steidel (1993)	Lin & Zou (2001)
Petitjean & Bergeron (1990)	Steidel <i>et al.</i> (1994)	Bond <i>et al.</i> (2001b)
Boissé <i>et al.</i> (1992)	Bowen <i>et al.</i> (1995)	<b><u>Ionization Conditions</u></b>
Steidel & Sargent (1992)	Steidel (1995)	Bergeron & Stasińska (1986)
Aldcroft <i>et al.</i> (1994)	Guillemin & Bergeron (1997)	Bergeron <i>et al.</i> (1994)
Malhotra <i>et al.</i> (1997)	Bouché <i>et al.</i> (2004)	Dittmann & Köppen (1995)
Churchill <i>et al.</i> (1999b)	Ménard <i>et al.</i> (2005)	Churchill & Le Brun (1998)
Rao & Turnshek (2000)	<b><u>Gas Kinematics</u></b>	Churchill <i>et al.</i> (2003)
Churchill & Vogt (2001)	Lanzetta & Bowen (1992)	<b><u>Multiphase Kinematics</u></b>
Churchill <i>et al.</i> (2003)	Churchill <i>et al.</i> (1996)	Churchill & Charlton (1999)
Ellison <i>et al.</i> (2004)	Churchill <i>et al.</i> (1999a)	Rigby <i>et al.</i> (2002)
Nestor <i>et al.</i> (2005)	Churchill <i>et al.</i> (2000b)	Charlton <i>et al.</i> (2003)
Prochter <i>et al.</i> (2005)	<b><u>Morphologies</u></b>	Ding <i>et al.</i> (2003)
<b><u>IR Studies</u></b>	Bowen <i>et al.</i> (1996)	Zonak <i>et al.</i> (2004)
Elston <i>et al.</i> (1996)	Steidel <i>et al.</i> (1997)	Masiero <i>et al.</i> (2005)
Kobayashi <i>et al.</i> (2002)	Steidel (1998)	Ding <i>et al.</i> (2005)
	Churchill <i>et al.</i> (2005)	
	Kacprzak <i>et al.</i> (2005)	
	<b><u>Gas+Gal Kinematics</u></b>	
	Steidel <i>et al.</i> (2002)	
	Ellison <i>et al.</i> (2003)	

### 2.1. Spectroscopic Surveys

The spectroscopic surveys are conveniently sub-divided into the ultraviolet (UV), optical, and infrared (IR) bands, since these probe distinct redshift regimes.

The UV surveys include an unbiased low redshift ( $z \leq 0.1$ ) MgII survey (Churchill 2001) and a study of the far-UV high ionization transitions (i.e., CIV, NV, OVI, etc.) and neutral hydrogen transitions (i.e., Ly $\alpha$ , Ly $\beta$ , etc.) associated with intermediate redshift MgII absorbers using the FOS spectrograph on board *HST* (Churchill *et al.* 2000a,b).

Several optical surveys have yielded a solid statistical picture of MgII absorbers at intermediate redshifts ( $0.3 \leq z \leq 2.2$ ). In the late 1980s and early 1990s, these surveys involved the slow methodical accumulation of quasar spectra with resolutions 1–2 Å and yielded some few hundred absorption systems (e.g., Lanzetta, Turnshek, & Wolfe 1987; Sargent, Steidel, & Boksenberg 1988b; Steidel & Sargent 1992). The equivalent width sensitivity of these surveys was typically 0.3 Å. With the advent of the Sloan Digital Sky

Survey (SDSS) mega-database, Nestor *et al.* (2005) and Prochter *et al.* (2005) cataloged several thousand MgII absorbers ripe for further study. However, the sensitivity is not uniform and hovers just below the  $1.0 \text{ \AA}$  level for the majority of the quasars.

An important quantity measured from these surveys is the redshift path density,  $dN/dz$ . In Figure 2 (left panel), the redshift path density is plotted for SDSS survey of Nestor *et al.* (2005) and the FOS *HST* survey of Churchill (2001). The solid curve is the no-evolution expectation ( $\Omega_m = 0.3, \Omega_\Lambda = 0.7$ ),

$$dN/dz = N(z)(1+z)^2[\Omega_m(1+z)^3 + \Omega_\Lambda]^{-1/2}, \quad (2.1)$$

fit to the binned data, where the dotted curves provide the range for  $3 \sigma$  uncertainty in the normalization,  $N(z)$ . The  $3 \sigma$  upper limit at  $z \sim 0.05$  (open point) assumes no evolution in the equivalent width distribution from the intermediate redshift data.

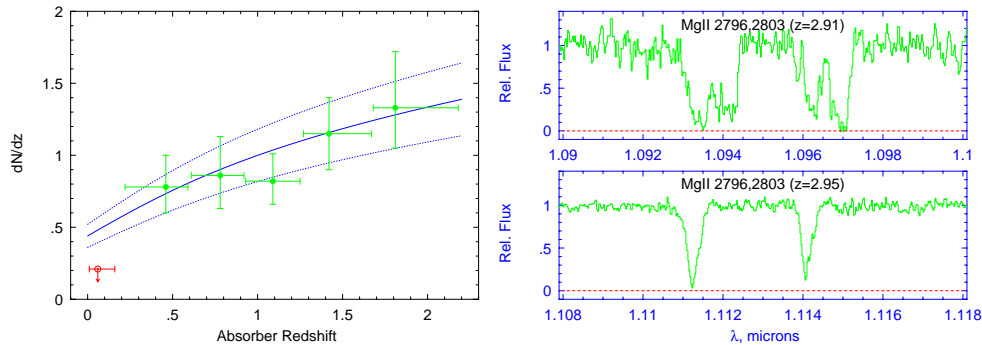


**Figure 2.** — (left) The redshift path number density of MgII absorbers with  $W_r \geq 0.3 \text{ \AA}$  as a function of redshift. The solid circles are from Nestor *et al.* (2005), and the open point (upper limit) is taken from Churchill (2001). — (right) Examples of  $z \sim 3$  MgII systems discovered in our in-progress survey of higher redshift MgII absorbers using the IRCS on Subaru. The velocity resolution is  $\Delta v \simeq 45 \text{ km s}^{-1}$  in the absorber rest frame.

A first glimpse of the MgII absorber kinematics was provided by Petitjean & Bergeron (1990) at a resolution of  $\Delta v \sim 30 \text{ km s}^{-1}$ . With the advent of HIRES (Vogt *et al.* 1994) on the Keck I telescope, Churchill & Vogt (2001) were able to resolve the kinematics of MgII absorption at  $\Delta v \sim 6 \text{ km s}^{-1}$ . These data also allowed Churchill *et al.* (1999b) to probe to a sensitivity of  $\sim 0.02 \text{ \AA}$ , which uncovered the large population of “weak” MgII absorbers. A low-end cut off in the MgII equivalent width distribution is yet to be observed.

Charting the properties of MgII absorbers at  $z > 2.2$  requires IR spectroscopy. In the IR, the present status is similar to that of optical surveys in the late 1980s and early 1990s. Recently, surveys of MgII absorbers have become possible using IR spectrographs, but the work is slow. In collaboration with Naoto Kobayashi, we have accumulated  $\sim 35$  high redshift quasars for a survey of  $2.5 \leq z \leq 4.0$  MgII absorbers. In Figure 2 (right panel), two examples of the  $z \sim 3$  MgII absorbers are shown. We are using NICFPs on the 3.5-meter telescope at the Apache Point Observatory to image the quasar fields to survey for the absorbing galaxies at  $2.5 \leq z \leq 4.0$ .

## 2.2. The Absorber–Galaxy Connection

Studies of the galaxies include surveys of the quasar fields, both targeted and statistical, and targeted studies of the absorbing gas kinematics, the galaxy morphologies, and the connections between the galaxy kinematics and the gas kinematics.

The nature of luminous objects associated with MgII absorbers was an open debate in the early 1990s. The work of Yanny (1990) favored a picture in which star forming sub-galactic fragments at impact parameters of 100–200 kpc gave rise to MgII absorption. However, this was at a time when some scenarios suggested that  $z \sim 0.2$  was an epoch of active galaxy formation via sub-galactic fragments. The seminal work of Bergeron & Boissé (1991) strongly suggested the presence of a bright,  $\sim L^*$  galaxy within a few tens of kpc from the absorbing gas. Soon after, Steidel, Dickinson, & Persson (1994) (hereafter, SDP94) firmly established the work of Bergeron & Boissé (1991) and reported the gross properties of the galaxies, including their rest-frame  $B - K$  colors, and  $L_B$  and  $L_K$  luminosity functions. Steidel (1995) presented a statistical picture of the luminosity dependent gas cross sections of MgII absorbing galaxies that has guided our conventional wisdom to the present.

The Steidel (1995) results are worth additional discussion. In Figure 3 (left panel) the impact parameters are plotted versus  $K$  luminosity for galaxies selected by  $W_r \geq 0.3 \text{ \AA}$  MgII absorption. Absorbing galaxies are plotted as solid circles and non-absorbing galaxies, based upon “control” fields, are plotted as open points. The dashed line was obtained by minimizing the number of non-absorbers above the line and minimizing the number of absorbers below the line. Using these results, Steidel (1995) inferred that the “halo” size of the galaxies scales as

$$R(L_K) = 38h^{-1} (L_K/L_K^*)^{0.15} \text{ kpc}, \quad (2.2)$$

that they have near unity covering factor, and that they must be roughly spherical in shape. It is otherwise difficult to explain the lack of non-absorbers below the  $R(L)$  relation of Eq. 2.2. Based upon semi-analytical and Monte-Carlo modeling, Lin & Zou (2001) infer that the value of the slope,  $\beta = 0.15$ , may in fact be steeper due to a limiting magnitude selection effect in the survey. We will revisit these inferences in § 3.

The redshift path density normalization,  $N(z)$ , constrains the product of the number density,  $n(z)$ , and cross section,  $\sigma(z)$ , that is  $N(z) = n(z)\sigma(z)$ . Using the  $K$  luminosity function of SDP94 for an estimate for  $n(z)$  and applying Eq. 2.2 for the gas cross section

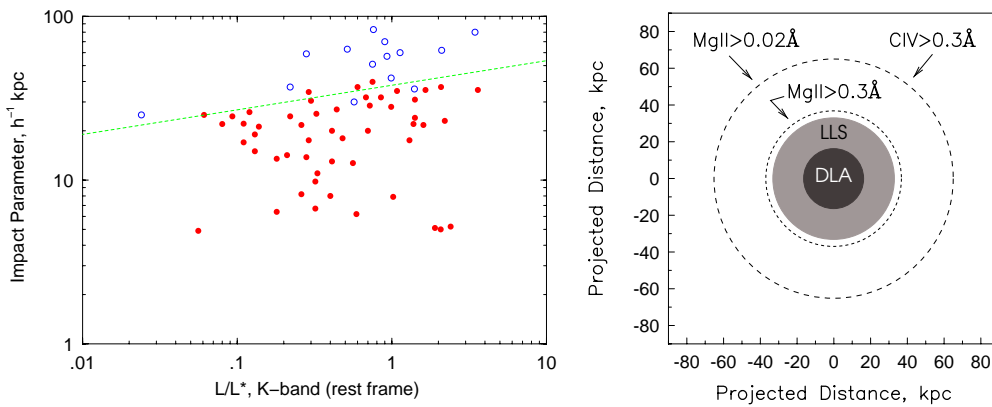


**Figure 3.** — (left) Galaxy-quasar impact parameter versus galaxy  $K$  luminosity for  $W_r \geq 0.3 \text{ \AA}$  (adapted from Steidel 1995). The solid points are absorbing galaxies and the open points are non-absorbers taken from “control” fields. The linear relationship is Eq. 2.2. — (right) The statistical cross section of various classes of absorbers, including DLAs, LLS, strong and weak MgII absorbers, and CIV systems.

provides a convenient formalism for the “halo” size of an  $L^*$  galaxy,

$$R_* = \left[ \frac{\pi c f_c \Phi^*}{H_o} \frac{(dX/dz)}{(dN/dz)} \Gamma(2\beta - \alpha + 1, L_{min}) \right]^{-1/2}, \quad (2.3)$$

where  $dN/dz$  is measured,  $f_c = 1$  is the assumed covering factor,  $\Gamma$  is the incomplete Gamma function,  $\Phi^* = 0.03h^3 \text{ Mpc}^{-3}$  and  $\alpha = -1$  are the normalization and faint-end slope of the galaxy luminosity function,  $\beta = 0.15$  is the slope of the  $R(L_K)$  relation,  $L_{min} = 0.05L_K^*$  is the faint-end cut off for galaxies giving rise to absorption, and  $dX/dz$  is the differential absorption distance,  $dX/dz = (1+z)^2 / \sqrt{\Omega_m(1+z)^3 + \Omega_\Lambda}$ , which is proportional to the probability of intercepting an absorber per unit redshift in a pencil beam survey.

In Figure 3 (right panel),  $R_*$  is shown for various regimes of  $N(\text{H I})$  associated with MgII absorbers, including DLAs, LLS, and strong and weak MgII absorbers. For strong MgII absorbers,  $R_* \simeq 40h^{-1} \text{ kpc}$  and for weak MgII systems  $R_* \simeq 70h^{-1} \text{ kpc}$ . Note that, statistically, LLS and strong MgII systems appear to be drawn from the same population. For comparison, CIV selected absorber sizes are also shown (e.g., Sargent, Steidel, & Boksenberg 1988a). Nestor *et al.* (2005) has performed a more sophisticated analysis, presenting  $R_*$  as a function of redshift for a variety of equivalent width cut offs.

A comparison of the gas kinematics and gross properties of the galaxies was pioneered by Lanzetta & Bowen (1992), and later expanded upon by Churchill, Steidel, & Vogt (1996), and Churchill *et al.* (1999a, 2000b). However, the sample size remained relatively small, at  $\sim 15$  galaxies, and no significant correlations were found. Little effort could be applied to establishing the nature of galaxies associated with weak MgII absorbers since the galaxies studied were originally selected from surveys with equivalent width sensitivities of  $W_r \geq 0.3 \text{ \AA}$ . However, both the fact that weak MgII absorbers are sub-LLS systems (Churchill *et al.* 2000a; Rigby *et al.* 2002) and the apparent lack of obvious bright, normal galaxy candidates in the studied fields (Churchill *et al.* 1999b) allowed for speculation that weak MgII absorbers were probably associated with LSB and/or dwarf galaxies at large impact parameters or isolated star forming pockets in the intergalactic medium (Churchill & Le Brun 1997; Rigby *et al.* 2002; Zonak *et al.* 2004).

*HST* has obtained images of roughly three-dozen quasar fields with known MgII absorbers. The images, most of them obtained using WFPC-2 with the F702W filter, provide a few to several kiloparsec resolution of intermediate redshift galaxies approximately at their rest-frame  $B$  band. Only a single quasar field, 3C 336, has been thoroughly studied in that the majority of galaxies within  $50''$  of the quasar have been spectroscopically redshifted (Steidel *et al.* 1997).

A direct comparison of the galaxy kinematics and the MgII absorption kinematics has been performed for only six galaxies to date (Steidel *et al.* 2002; Ellison, Mallén-Ornelas, & Sawicki 2003). The galaxies have been carefully selected; each a nearly edge-on spiral with the disk major-axis intersecting the quasar line of sight (though beyond the visible extent of the disk). In the Steidel *et al.* (2002) sample, four of the five galaxies have MgII absorbing gas that traces the rotation curve. Simplistic models suggest that the gas “halo” corotates with the galaxy, but that the halo rotation lags the galaxy rotation with height above the disk. Lagging halos are observed in local galaxies using 21-cm emission (Sancisi *et al.* 2001) and diffuse ionized gas emission (Swaters, Sancisi, & van der Hulst 1997; Rand 2000). In the fifth galaxy, the absorption is a narrow weak MgII component aligned at the galaxy systemic velocity. Ellison *et al.* (2003) found a different result; some of the MgII absorption is aligned with the galaxy rotation, but the majority of the gas lies at negative velocities with respect to the galaxy. Their result is analogous

to the “forbidden gas” observed in 21-cm studies of local galaxies (Fraternali *et al.* 2002). Ellison *et al.* favor a scenario in which superbubbles give rise to the MgII absorbing gas in the lower halo of the galaxy (also see Bond *et al.* 2001a).

This latter type of study holds the greatest promise for understanding the spatial and kinematic relationship between galaxies and their extended gaseous components. If we are to place constraints on scenarios and models of galaxy evolution using quasar absorption lines, it is imperative that a wide range of galaxy–quasar line-of-sight orientations are studied in tandem with the galaxy kinematics.

### 2.3. Modeling and Ionization Conditions

Modeling the geometric structure and ionization conditions of MgII “halos” began in earnest when the connection between galaxies was first being established observationally (Gruenwald & Viegas 1993; Srianand & Khare 1993). Additional sophistication was applied by Mo & Miralda–Escudé (1996), who developed a two-phase model in which MgII halos are defined by the cooling radius of infalling gas. However, their models predict too few LLS/MgII absorbers at  $z > 2$ . Charlton & Churchill (1998) modeled the kinematic composition of MgII absorbers; they concluded that disk kinematics likely make a significant contribution to the absorption profiles.

Photoionization modeling has been applied to observational data by several teams, following the seminal work of Bergeron & Stasińska (1986). However, it was not until the STIS spectrograph on *HST* provided high resolution UV spectra of absorption kinematics from a wide range of ionization species, such as SiII, SiIV, CII, CIII, CIV, NII, NV, OVI, and neutral hydrogen, that multiphase photoionization could be modeled in detail (Charlton *et al.* 2003; Ding *et al.* 2003; Zonak *et al.* 2004; Masiero *et al.* 2005; Ding, Charlton, & Churchill 2005).

From these studies, it is now firmly established that MgII absorbers are accompanied by a range of multiphase ionization/kinematic conditions, including separate high ionization phases in which MgII absorption is absent to  $W_r \simeq 0.02 \text{ \AA}$ . Importantly, the neutral hydrogen arises in multiple phases, highlighting the need for careful application of the Lyman series and careful separation of the HI contributions to each phase.

## 3. Toward New Insights into MgII Absorbing Galaxies

In the early 1990s, intermediate redshift galaxy surveys were in their incipient stages and MgII absorption galaxy selection was a clear cut and competitive method for exploring the general evolution of galaxies to earlier epochs. One of the first luminosity functions of  $z \sim 0.6$  galaxies was established using MgII absorption selection (SDP94). During this period, it was always purported that the MgII absorption selection method held the additional potential of measuring the kinematic, ionization, and chemical conditions of the gas phases of galaxies. In terms of direct case-by-case studies of the galaxies, much of this potential remains unexplored.

In an effort to build a large database for direct comparisons of the galaxy morphologies and MgII absorption kinematics, we have undertaken a program incorporating high spatial resolution *HST* images of the quasar fields and HIRES and UVES spectra of the MgII absorption. We have been careful to include in our sample only those absorption-selected galaxies with *confirmed* spectroscopic redshifts. It is important to keep in mind that our overall picture of MgII absorption selected galaxies has been based upon a sample of 52 of which 70% have spectroscopic redshifts and 30% are candidates (SDP94). By only including *confirmed* galaxies, it is our aim to be sure to illuminate any possible bias that

may have influenced what can be inferred about MgII absorber covering factors, halo sizes and geometries, and associated galaxy properties (see Charlton & Churchill 1996).

The SDP94 survey method was to obtain spectroscopic redshifts of galaxies in an outward pattern from the quasar, selecting galaxies with magnitudes and colors consistent with their being at the absorber redshift. The method was very effective. However, it is always possible that galaxies with unexpected magnitudes and odd colors near the quasars or galaxies at large separation could have been missed in the survey. SDP94 also measured the properties of galaxies in 25 “control” quasar fields, which were selected by the *absence* of MgII absorbers with  $W_r \geq 0.3 \text{ \AA}$  in the quasar spectrum. In this way, they obtained the properties of “non-absorbing” galaxies. We discuss possible bias in this approach in § 4.

### 3.1. Our Sample

To date, we have 38 galaxies in our sample, 26 of which we also have HIRES and/or UVES spectra of the absorption. In some of our fields, more than one galaxy is at the absorber redshift. For now, we cannot be 100% certain that additional galaxies contribute to the absorption. Ultimately, it will be necessary to establish the redshifts of all galaxies to a fixed absolute magnitude and to a fixed angular separation from the quasar. We are exploring the technique of photometric redshifts in order to place first order constraints on the redshift distribution of galaxies in the *HST* fields.

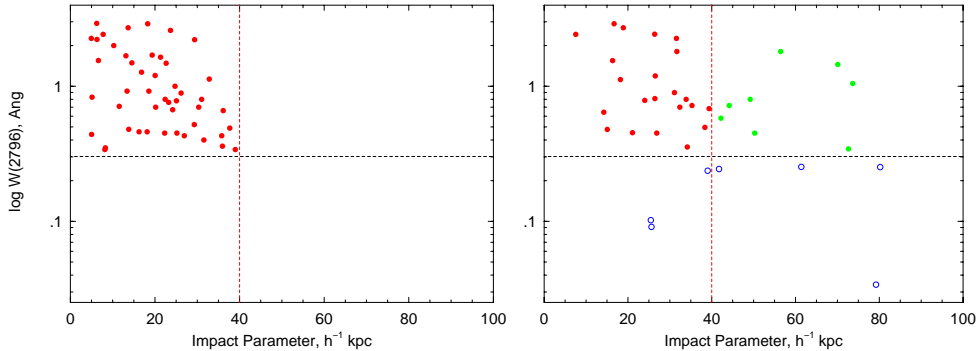


**Figure 4.** — The rest-frame MgII  $\lambda 2796$  equivalent widths versus impact parameters. The vertical dashed line marks  $D = 40 h^{-1}$ , the approximate value of  $R_*$ , and the horizontal dashed line is at  $W_r = 0.3 \text{ \AA}$ , the separation between strong and weak MgII absorbers. — (left) The upper left area is the region previously explored by Steidel, Dickinson, & Persson (1994). — (right) Our *HST* sample (to date).

Those caveats having been stated, we have found some generally illuminating results that are *not* sensitive to incompleteness of redshifts in the quasar fields. In Figure 4, we show the distribution of equivalent widths versus galaxy impact parameter. In the left panel, we show the original SDP94 distribution for  $W_r > 0.3 \text{ \AA}$ . To guide the eye, we have placed a vertical line at  $D = 40 h^{-1} \text{ kpc}$  approximately at the  $R_*$  value. We have also placed a horizontal line at  $W_r = 0.3 \text{ \AA}$  to demarcate “strong” and “weak” MgII absorbers. Note that the SDP94 survey data lie exclusively in the range  $D < 40 h^{-1} \text{ kpc}$  and  $W_r > 0.3 \text{ \AA}$ †.

† A few of the galaxies published in the SDP94 paper have  $W_r > 0.2 \text{ \AA}$ ; however, these



In the right panel of Figure 4, we show our *HST* sample (to date). Our sample includes 38 absorption systems. In cases where we have HIRES and UVES spectra, the equivalent widths have been remeasured. We have also remeasured the galaxy–quasar impact parameters in the *HST* images. Though there is substantial overlap between our sample and the SDP94 sample, the new equivalent widths and impact parameters do not always exactly match those measured in the lower resolution SDP94 data; this is simply a resolution effect.

As can be seen, we have found galaxies associated with weak absorbers over a wide range of impact parameters and galaxies with strong absorbers well beyond the  $R_*$  prediction. The absorbers in the range  $70 \leq D \leq 80 h^{-1}$  kpc are particularly remarkable in that a wide range of equivalent widths are observed. At face value, it would appear that there are departures from our current conventional wisdom. The weak systems at  $D \leq 40 h^{-1}$  kpc immediately suggest that the extended gaseous regions surrounding galaxies are patchier than previously reported. Moreover, the strong MgII absorbers at  $D \geq 40 h^{-1}$  kpc suggest that the absorbing gas geometry is less regular than previously reported. In § 3.4, we will highlight a few cases to illustrate that there are clear exceptions to our current expectations.

Since MgII equivalent width is strongly proportional to the velocity spread and number of components, or “clouds” (Petitjean & Bergeron 1990; Churchill *et al.* 2003), these data suggest that the kinematic conditions of the absorbing gas is not strongly connected to the projected separation from the galaxy (also see Churchill *et al.* 1996).

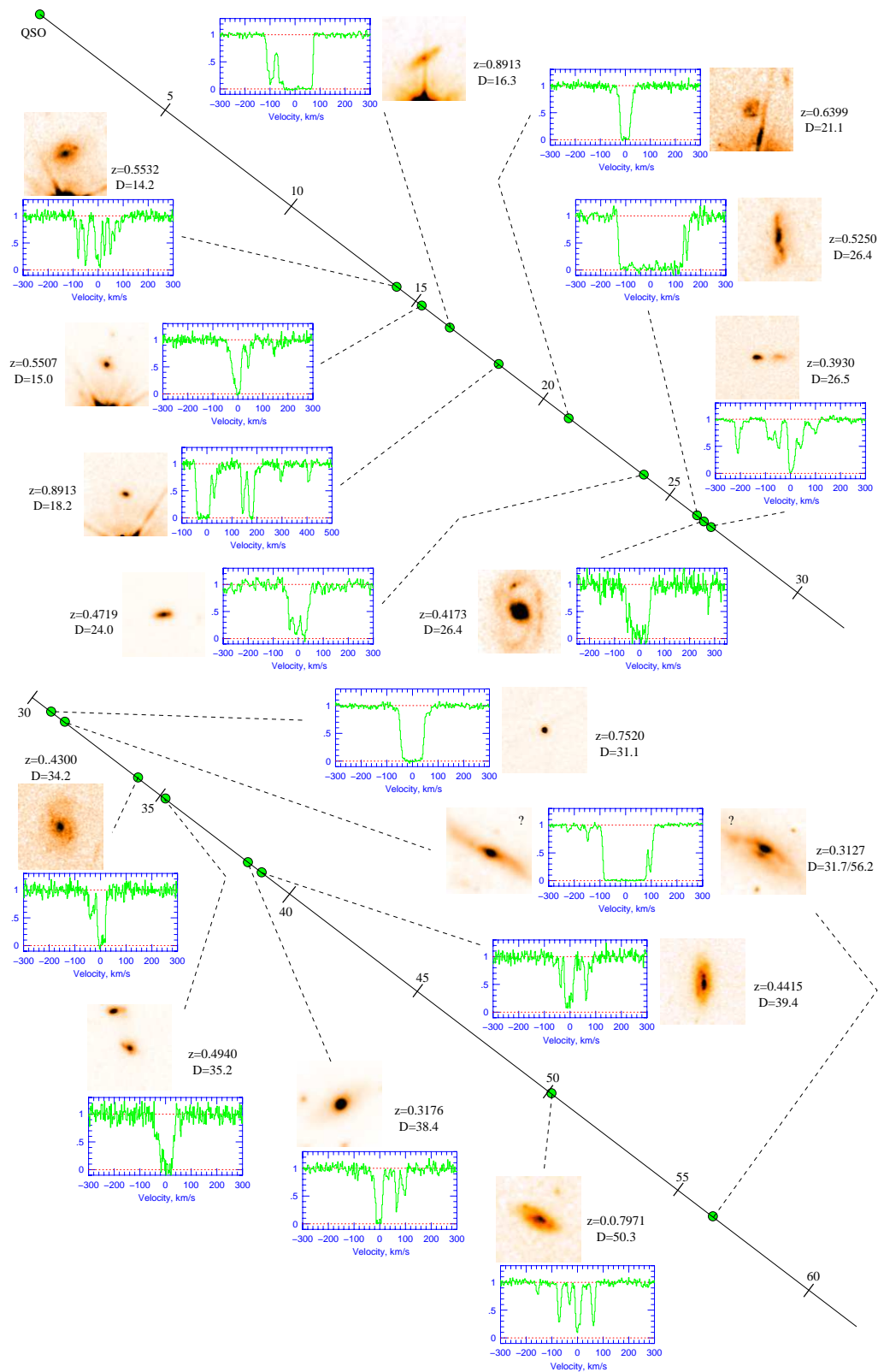
### 3.2. Morphologies, Orientations, and Gas Kinematics

In Figure 5, we present our current sample having  $W_r > 0.3 \text{ \AA}$ . For each galaxy, the *HST* image of the absorbing galaxy is  $5'' \times 5''$  and oriented such that the quasar is downward. This orientation provides a consistent galaxy–quasar line of sight orientation for all galaxies for purposes of illustration. The HIRES and UVES absorption profiles are of the MgII  $\lambda 2796$  transition only, shown in rest-frame velocity space over an interval of  $\Delta v = 600 \text{ km s}^{-1}$ . The velocity zero point is unrelated to the galaxy redshift; for each profile, the zero point is the optical depth median of the absorption. The galaxies are presented in order of increasing impact parameter. An “impact parameter ruler” runs from the upper left to the lower right of each panel (first)  $0 \leq D \leq 30 h^{-1}$  kpc, (second)  $30 \leq D \leq 60 h^{-1}$  kpc, and (third)  $60 \leq D \leq 90 h^{-1}$  kpc.

Based upon a visual examination, we can see that MgII absorption selected galaxies are, as a whole, fairly normal looking. Most galaxies are spiral galaxies. However, closer inspection reveals that the majority of the galaxies have minor perturbations, and in some cases what appears to be bright HII regions and/or minor companions. There is no trend between galaxy morphological type with impact parameter. Inspection of the MgII absorption reveals a wide variety of kinematics. Interestingly, there are DLA/HI-rich absorbers at both small and very large impact parameters.

The galaxy orientation provides the light path geometry through the galaxy, where the impact parameter is the closest approach to the galactic center. By orientation, we mean the combined projection of the galaxy due to the galaxy inclination,  $i$ , and the position angle,  $\phi$ , of the galaxy. We define the position angle as the primary angle between the galaxy major axis and a line connecting the galaxy center and the quasar. As a reminder, all galaxies are oriented such that the quasar is located downward in Figure 5.

We have used GIM2D (Simard *et al.* 2002) to model the galaxy morphologies, and from systems were found *after the fact*, in that a potential absorbing galaxy was observed in the quasar field and then MgII absorption was sought in follow-up, deeper quasar spectra.



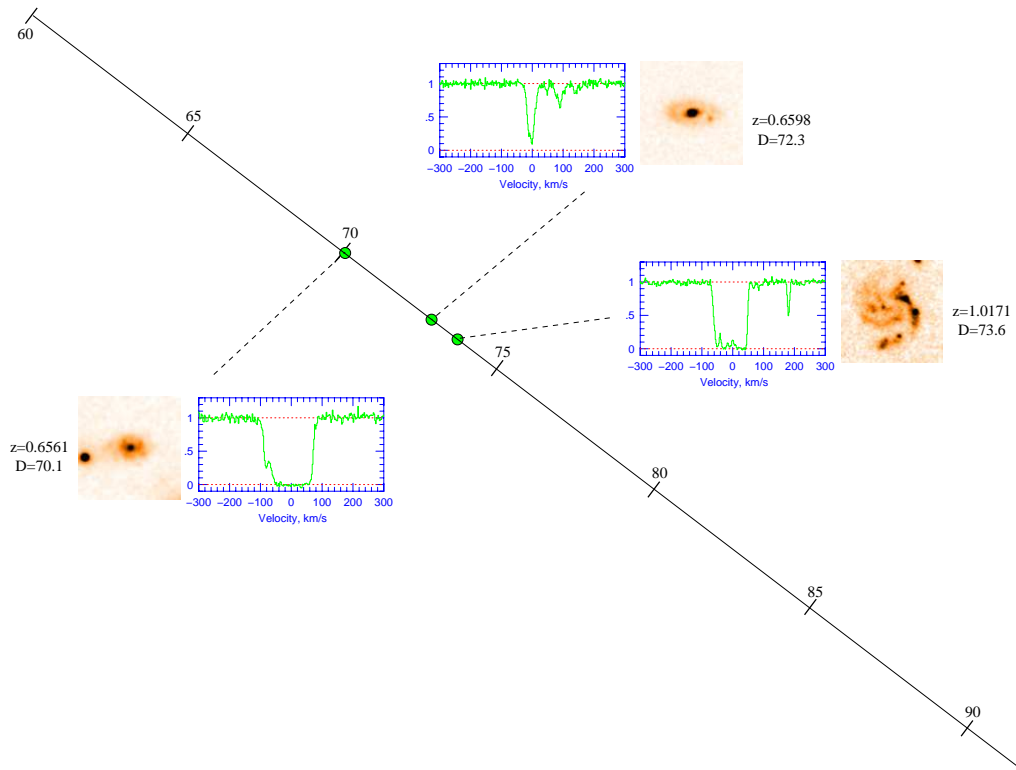


**Figure 5.** *HST* images and HIRES/UVES MgII  $\lambda 2796$  profile of absorbing galaxies displayed in order of increasing impact parameter,  $D$ , for the range  $0 \leq Dh \leq 90 h^{-1}$  kpc. For the small impact parameter systems, the diffraction spikes from the quasar can be seen. The axis running from upper left serves as an “impact parameter ruler”. The images are  $5'' \times 5''$  and oriented such that the quasar is downward in order to illustrate the galaxy orientation with respect to the quasar line of sight. The absorption profiles are shown in rest-frame velocity space over an interval of  $\Delta v = 600 \text{ km s}^{-1}$ , where the zero point is arbitrarily defined.

these models measure the galaxy position angles and inclinations (details in Kacprzak *et al.* 2005, *this volume*). These are two-component (bulge and disk), axis-symmetric, smooth models. As such, perturbations in the galaxy morphologies are clearly present in the residuals and can be quantified. We find significant departures from smooth morphologies in MgII absorbing galaxies that would otherwise be missed without modeling.

We have searched for correlations between galaxy orientation parameters and MgII absorption properties. Galaxy orientation parameters (such as  $\cos \phi$ ,  $\sin \phi$ ,  $\cos i$ ,  $\sin i$ ,  $\cos \phi \cos i$ ,  $\sin \phi \cos i$ , etc.), do not correlate with absorption properties. This might be interpreted to mean that the halos are spherical; however, it can just as well be interpreted to mean that the absorbing gas can be extended in any orientation with respect to the galaxy. For the latter scenario to be favored, we would expect very weak to non-absorption at moderate impact parameters in some fraction of the galaxies. We will show below that this is precisely what we are finding. Interestingly, we find a  $3.2 \sigma$  correlation between the MgII  $\lambda 2796$  equivalent width and the galaxy morphological “asymmetries” normalized by the impact parameter. The details and interpretations are discussed in Kacprzak *et al.* (*this volume*).

### 3.3. Weak Systems and Galaxies

In our sample, there are seven weak MgII systems for which we have *HST* images of the quasar fields. Follow up spectroscopy has revealed, in each case, that weak systems are associated with galaxies. Furthermore, these galaxies appear to have fairly normal morphologies, if somewhat sub- $L^*$  luminosities. This suggests that weak MgII absorbers do not select a particular class of galaxy (i.e., LSB, dwarf) or post-star forming object.

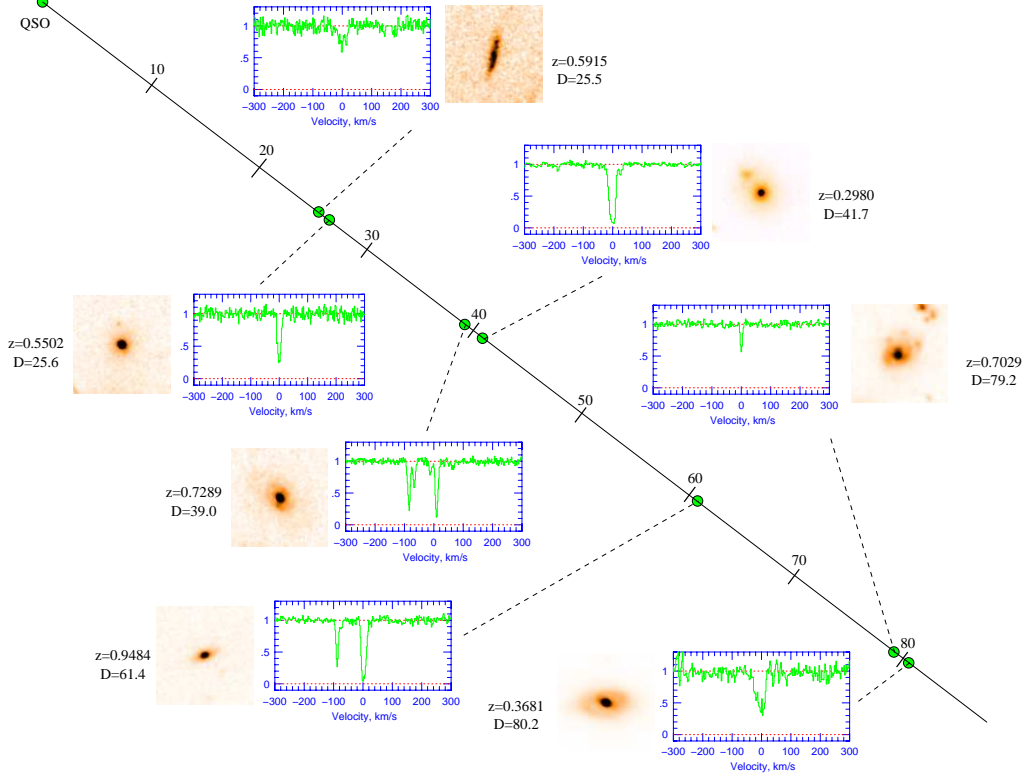


**Figure 6.** Same as Figure 5 but for the weak MgII absorbers (defined to have  $W_r < 0.3 \text{ \AA}$ ) over the range  $0 \leq D \leq 80 h^{-1} \text{ kpc}$ . We have found seven weak MgII absorbers clearly associated with galaxies.

Two of the seven galaxies are at impact parameters  $D h^{-1} \simeq 80 \text{ kpc}$ . On the other hand, three (almost four) of the seven galaxies are at  $D h^{-1} \leq 40 \text{ kpc}$ , and would have been labeled as non-absorbing galaxies in the SDP94 survey. In fact, in two cases, the galaxy at the weak MgII absorption redshift was misidentified to be associated with strong MgII absorption at a different redshift due to the lack of spectroscopic redshifts. Such reidentifications imply that the covering factor for  $W_r > 0.3 \text{ \AA}$  is probably less than unity (see Charlton & Churchill 1996).

We cannot yet constrain the distribution of impact parameters for weak systems; to do so would require a larger sample. However, if we consider that we have observed two absorbers at  $D h^{-1} \geq 70 \text{ kpc}$  that classify as DLA/HI-rich and three weak absorbers at  $D h^{-1} \leq 40 \text{ kpc}$ , we would probably be incorrect to assume that weak MgII absorbers are preferentially found at large impact parameters and stronger absorbers are found only at smaller impact parameters. As such, we may be finding that weak MgII absorption arises in galaxies with a distribution of impact parameters similar to that of strong

MgII absorbers. For this to be the case, the  $N(\text{H I})$  around the galaxies must range over several orders of magnitude at all impact parameters (probably becoming more varied with increasing impact parameter).

### 3.4. More to the Story?

In Figures 7 and 8, we show two quasar fields that further suggest that MgII absorption is patchier than previously thought. If the examples of these fields are moderately common, it would require modification of our current views.

In the Q1222 + 228 field, the first absorber known was at  $z = 0.6681$ . The MgII profiles are shown in the lower right of Figure 7. It is a strong absorber easily detected in the spectrum of Steidel & Sargent (1992). The edge-on spiral galaxy at  $D \simeq 26 h^{-1}$  kpc, labeled in the *HST* image of Figure 7, was assumed to be the host of the MgII absorption. However, a LRIS/Keck I spectrum of the galaxy places it at  $z = 0.5502$ , a redshift at which Churchill *et al.* (1999b) previously reported a weak MgII absorber. The strong  $z = 0.6681$  MgII absorbing galaxy remains unidentified. As labeled in Figure 7, there are six candidate galaxies, G1–G6, for the  $z = 0.6681$  MgII absorber. At this redshift, they lie in the impact parameter range  $63 \leq D \leq 108 h^{-1}$  kpc, which is well beyond the  $R_*$  expectation (shown by the dashed circle centered on the quasar). We are in the process of obtaining the spectra of these six galaxies; if/when the absorber is identified, it may yet be another example of strong absorption at large impact parameter.

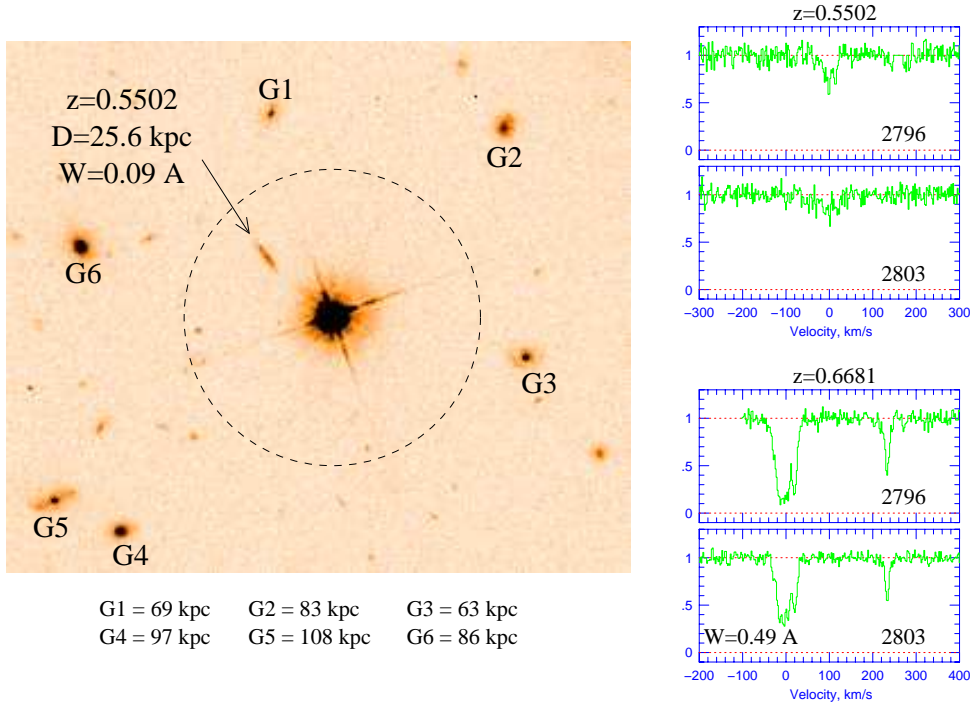


**Figure 7.** — (left) The WFPC-2 *HST* image of the Q1222+228 field. The  $z = 0.5502$  absorbing galaxy is identified; it is a weak MgII absorber. There is strong MgII absorption at  $z = 0.6681$ , but the galaxy remains unidentified. Absorber candidates are labeled G1 through G6, but they all lie outside of the  $R_*$  prediction shown as the dashed circle centered on the quasar. — (right) The HIRES absorption profiles for the  $z = 0.5502$  and  $z = 0.6681$  systems. The absorption profiles are shown in rest-frame velocity space over an interval of  $\Delta v = 600 \text{ km s}^{-1}$ , where the zero point is arbitrarily defined.

As seen in Figure 8, a bright  $z = 0.6720$  galaxy with  $D \simeq 41 h^{-1}$  kpc in the Q1317+274 field is a classic example of the type of galaxy expected to host strong MgII absorption. However, at the expected location of the MgII doublet in the HIRES spectrum, we find no absorption to a  $3\sigma$  limit of  $W_r < 0.006 \text{ \AA}$  (upper right panel). This limit is a factor of three below current surveys for weak MgII absorbers and a factor of 50 below the expected absorption strength for this galaxy. For MgII, this “mother of all non-absorbers” provides an emphatic accentuation to our other findings that the halos around galaxies are quite patchy and that the covering factor for  $W_r > 0.3 \text{ \AA}$  and  $D \leq 40 h^{-1}$  kpc must be less than unity.

In the Q1317 + 274 field, there is MgII absorption at  $z = 0.6610$  with  $W_r = 0.34 \text{ \AA}$ . The profiles are shown in the lower right of Figure 8. The absorption is associated with a bright galaxy at  $D \simeq 72 h^{-1}$  (see Steidel *et al.* 2002). This latter galaxy would not be expected to give rise to absorption with this equivalent width. This example suggests that the geometry of galaxy “halos” is not necessarily spherical, but can apparently be highly extended.

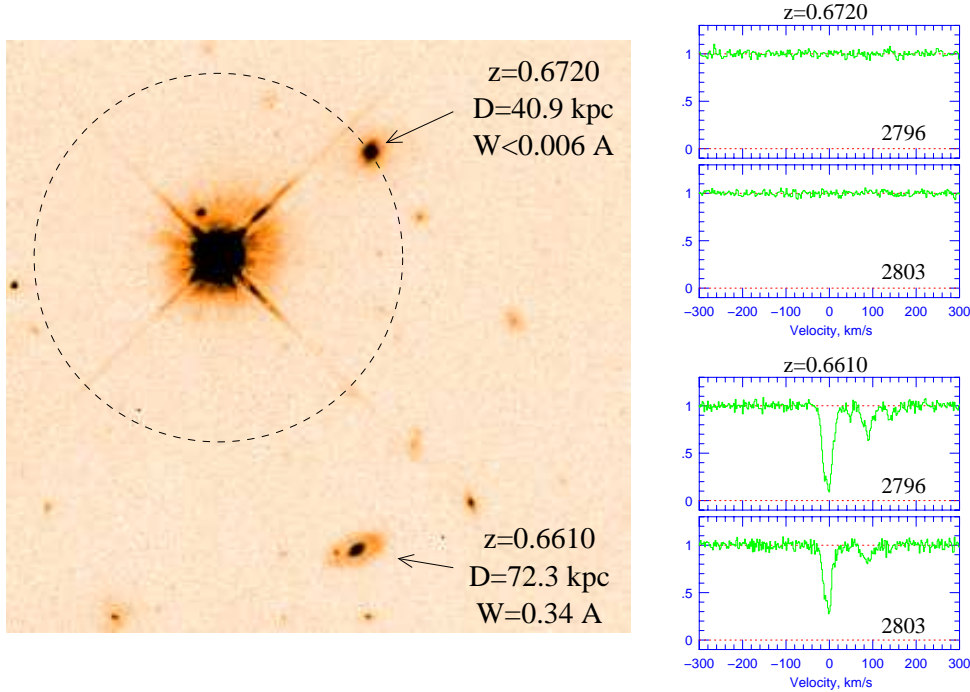


**Figure 8.** — (left) The WFPC-2 *HST* image of the Q1317+274 field. The  $z = 0.6610$  absorbing galaxy is at  $72 h^{-1}$  kpc, well outside the  $R_*$  prediction, shown as a dashed circle centered on the quasar. A second galaxy at  $41 h^{-1}$  kpc, is confirmed to have  $z = 0.6720$ . — (right) The HIRES/Keck absorption profiles for the  $z = 0.6610$  systems (lower) and the HIRES spectrum at the expected location of the  $z = 0.6720$  galaxy. There is no absorption to a rest-frame limit of  $W_r \leq 0.006 \text{ \AA}$  ( $3\sigma$ ).

In our sample, there are two absorbers that arise in “double” galaxies (see Figure 5). The first is at redshift  $z = 0.4940$  with an approximate impact parameter of approximately  $D = 35.2 h^{-1}$  kpc (galaxy nearest the quasar). These galaxies appear to be in the process of merging, for there is a tidal tail attached to each galaxy that arcs back toward its companion. Note however, that the absorption does not have the tall-tale signs of a

“double” MgII absorber (Churchill *et al.* 2000b) based upon the less than 200 km s<sup>-1</sup> velocity spread and absence of high velocity kinematic subsystems.

The second pair is at  $z = 0.3127$ . One is at  $D = 35.2 h^{-1}$  kpc and the second is at  $D = 56.2 h^{-1}$  kpc. The projected separation between the galaxies is only 36.5  $h^{-1}$  kpc, but it is not clear if they are gravitationally bound or part of a group. Originally, the closer in galaxy was assumed to be the only absorber. This case illustrates that additional care must be taken to acquire a full census of the galaxies in absorber fields (also see Bowen, Blades, & Pettini 1995). Interestingly, both galaxies have almost identical orientations with respect to the quasar line of sight. There appears to be a warped disk in the  $D = 35.2 h^{-1}$  kpc galaxy and perhaps some disturbance and LMC/SMC-like satellite galaxies associated with the  $D = 56.2 h^{-1}$  kpc. It may be that one can never establish the host galaxy of the absorption for such cases; however, obtaining the kinematics of the galaxies themselves (i.e., rotation curves) would serve to constrain the dynamical relationships between the galaxies and the absorption.

#### 4. Sorting it Out

We have shown several galaxies where the impact parameters and strengths of MgII absorption run counter to our current conventional wisdom. Our data would suggest a covering factor for  $W_r > 0.3 \text{ \AA}$  less than unity (how much less we cannot say) and a geometry that is not necessarily characterized as spherical.

In order to firmly establish the character of MgII absorbing gas connected to galaxies we must quantify the covering factor and extent of the absorption as a function of absorption strength and galaxy properties. However, any survey *must* include the distribution of very weak and non-absorbing galaxies. Due to the sensitivity of HIRES and UVES quasar spectra, the definition of a non-absorbing galaxy can now be based upon equivalent width limits of  $W_r \simeq 0.02 \text{ \AA}$ , a factor of 15 below previous surveys. It is imperative that the cataloging of galaxies in quasar fields be complete to a limiting absolute magnitude and to a fixed projected physical separation from the quasar.

It is not clear that the use of control fields (those in which no MgII absorption is seen in the quasar spectra) is the best approach to cataloging non-absorbing galaxies. It is quite possible that the majority of these quasars could lie in the direction of sparse galaxy fields so that the galaxies would preferentially be at large impact parameters. Because the quasars are known *a priori* to lack absorption, it is also possible that control fields could preferentially select galaxies with “special” histories that yield highly patchy halos or small halo geometries. These considerations may partially explain the lack of non-absorbing galaxies at small impact parameters reported by Steidel (1995). On the contrary, most quasar with MgII absorption have several galaxies in their fields. There is no reason to suppose that, on average, a galaxy in a field with other absorbers at different redshifts would preferentially be a non-absorbing galaxy.

It can be argued that the whole methodology of galaxy selection should be turned around; quasar fields should be surveyed for galaxies before any knowledge of absorption in the quasar spectra. However, the galaxy morphologies are a keystone ingredient to these studies and it would be difficult to successfully motivate wholesale *HST* imaging of such fields. Obtaining *HST* images of fields with known absorbers guarantees some galaxies for galaxy-absorber connection analysis and provides morphologies of galaxies that classify as non-absorbers.

In the end, it will be studies which incorporate both the galaxy kinematics and the absorption kinematics that hold the greatest promise for promoting our understanding of the nature of extended gaseous regions associated with galaxies.

## 5. Conclusions

We have presented a brief history and review of MgII absorption selected galaxies. In addition, we have presented new results and inferences regarding the nature of MgII absorbing gas in the vicinity of galaxies. Our data include high spatial resolution *HST* images of the quasar fields and HIRES and UVES high velocity resolution spectra of the absorbing gas. We have carefully confirmed the redshifts of all galaxies in our sample to be coincident with the absorption redshifts. Our sample, to date, comprises 38 *HST* imaged MgII absorbing galaxies, 26 of which we also have HIRES and/or UVES spectra of the MgII absorption. We are currently working to obtain the HIRES and UVES spectra for the remaining 12 absorbers. We summarize our main points below:

(a) The extended gaseous envelopes surrounding intermediate redshift galaxies are more patchy than previously reported. Our survey data are suggestive that the MgII absorbing galaxy “halos” have a covering factor less than unity and geometries that depart from spherical. A complete and unbiased survey of quasar fields using *HST* images and high-resolution quasar spectra are required to quantify these statements.

(b) We have made first steps toward quantifying the morphologies of galaxies hosting MgII absorption. From the galaxy orientations, we have constrained the quasar sightline paths through these galaxies. We have searched for correlations with MgII absorption properties, including velocity spread, velocity asymmetry, number of “clouds”, equivalent width, doublet ratio, and total column density. There are no significant correlations between galaxy orientation and gas kinematics, suggesting that the halo geometries and gas velocity fields are, in general, not strongly linked to those of the galaxies.

(c) Some (and possibly the majority) of weak MgII absorbers are associated with normal galaxies over a range of impact parameters. We have found direct association in seven of seven cases for which we have obtained the spectroscopic redshifts of the candidate galaxies. This suggests that weak MgII absorbers do not select a particular class of galaxy (i.e., LSBs, dwarfs, etc.) or post-star forming object.

We have emphasized the importance of a complete survey of galaxies in quasar fields to a fixed absolute magnitude and fixed galaxy–quasar separation. It is vital that we know the redshifts of both absorbing and non-absorbing galaxies in the fields in order to quantify the covering factor and constrain the geometry of the absorbing gas. Since our absorption line spectra are sensitive to  $W_r \simeq 0.02 \text{ \AA}$  (and even better in some cases), we will be able to examine these issues to a higher level of sensitivity than previous studies. In our survey, a non-absorbing galaxy will be one where the limits on MgII absorption is roughly a factor of ten more sensitive than the previous  $W_r < 0.3 \text{ \AA}$  criterion. Such a survey of the quasar fields will be very time intensive and will require systematic and long-term effort. We are exploring the possibility of using photometric redshifts to place first-order constraints on the galaxies in these fields.

What we wish to emphasize even more strongly is the need to obtain high quality spectra of the galaxies known to host MgII absorption. In particular, it is vital that we obtain accurate redshifts (with uncertainties less than  $\simeq 20 \text{ km s}^{-1}$ ). This will allow us to constrain the relative velocities of the gas and the galaxy. Most desirable are rotation curves for the galaxies in order to extend the studies of Steidel *et al.* (2002) and Ellison *et al.* (2003). We now have a reasonably sized sample and can examine the kinematic connections between galaxies and MgII absorption for a wide variety of galaxy orientations and galaxy kinematics (once rotations curves are obtained).

It is a detailed case-by-case study of the galaxy kinematics – absorbing gas kinematics connections that hold the greatest promise for constraining the role of gas in galaxy evolution. These are the data that will ultimately provide the most meaningful constraints on



galaxy–galaxy halo models (which will soon incorporate mock spectra in a manner similar to cosmological simulations). We can constrain the line-of-sight light path through the galaxies; however, only by documenting the velocities of the gas relative to those of the galaxies can we compare the observed conditions in early epoch galaxies to models of galactic fountains, superbubbles, galactic winds, high velocity clouds, and accretion via minor mergers. This is how we will finally understand the nature of extended gaseous envelopes around normal galaxies.

### Acknowledgements

We would like to acknowledge partial support from NASA, the NSF, and the IAU. Naoto Kobayashi, Michael Murphy, Michael Rauch, Wal Sargent, and Alice Shapley all made important contributions to the new work presented herein.

### References

- Aldcroft, T.L., Bechtold, J., & Elvis, M. 1994, *ApJS*, 93, 1
- Bechtold, J., & Ellingson, E. 1992, *ApJ*, 396, 20
- Bergeron, J., & Stasińska, G. 1986, *A&A*, 169, 1
- Bergeron, J., & Boissé, P. 1991, *A&A*, 243, 344
- Bergeron, J., *et al.* 1994, *ApJ*, 436, 33
- Bond, N.A., Churchill, C.W., Charlton, J.C., & Vogt, S.S. 2001b, *ApJ*, 557, 761
- Bond, N.A., Churchill, C.W., Charlton, J.C., & Vogt, S.S. 2001b, *ApJ*, 562, 641
- Boissé, P., Boulade, O., Kunth, D., Tytler, D., & Vigroux, L. 1992, *A&A*, 262, 401
- Bowen, D.V., Blades, J.C., & Pettini, M. 1995, *ApJ*, 448, 634
- Bowen, D.V., Blades, J.C., & Pettini, M. 1996, *ApJ*, 472, 77
- Bowen, D.V., Tripp, T.M., & Jenkins, E.B. 2001, *AJ*, 121, 1456
- Bouché, N., Murphy, M.T., & Péroux, C. 2004, *MNRAS*, 354, L25
- Caulet, A. 1989, *ApJ*, 340, 90
- Charlton, J.C., & Churchill, C.W. 1996, *ApJ*, 465, 631
- Charlton, J.C., & Churchill, C.W. 1998, *ApJ*, 499, 181
- Charlton, J.C., Ding, J., Zonak, S.G., Churchill, C.W., Bond, N.A., & Rigby, J.R. 2003, *ApJ*, 589, 111
- Churchill, C.W. 2001, *ApJ*, 560, 92
- Churchill, C.W., & Charlton, J.C. 1999, *AJ*, 118, 59
- Churchill, C.W., & Le Brun, V. 1998, *ApJ*, 499, 677
- Churchill, C.W., Mellon, R.R., Charlton, J.C., Jannuzi, B.T., Kirhakos, S., Steidel, C.C., & Schneider, D.P. 1999a, *ApJ*, 519, L43
- Churchill, C.W., Mellon, R.R., Charlton, J.C., Jannuzi, B.T., Kirhakos, S., Steidel, C.C., & Schneider, D.P. 2000a, *ApJS*, 130, 91
- Churchill, C.W., Mellon, R.R., Charlton, J.C., Jannuzi, B.T., Kirhakos, S., Steidel, C.C., & Schneider, D.P. 2000b, *ApJ*, 543, 577
- Churchill, C.W., Rigby, J.R., Charlton, J.C., & Vogt, S.S. 1999b, *ApJS*, 120, 51
- Churchill, C.W., Steidel, C.C., & Kacprzak, G.G. 2005, in R. Braun (ed.), *Extraplanar Gas*, vol. 331, p. 387
- Churchill, C.W., Steidel, C.C., & Vogt, S.S. 1996, *ApJ*, 471, 164
- Churchill, C.W., & Vogt, S.S. 2001, *AJ*, 122, 679
- Churchill, C.W., Vogt, S.S., & Charlton, J.C. 2003, *AJ*, 125, 98
- Ding, J., Charlton, J.C., Bond, N.A., Zonak, S.G., & Churchill, C.W. 2003, *ApJ*, 587, 551
- Ding, J., Charlton, J.C., & Churchill, C.W. 2005, *ApJ*, 621, 615
- Dittmann, O.J., & Köppen, J. 1995, *A&A*, 297, 671
- Drinkwater, M.J., Webster, R.L., & Thomas, P.A. 1993, *AJ*, 106, 848
- Ellison, S., Churchill, C.W., Rix, S.A., & Pettini, M. 2004, *ApJ*, 615, 118
- Ellison, S., Mallén–Ornelas, G., & Sawicki, M. 2003, *ApJ*, 589, 709

- Elston, R., Bechtold, J., Hill, G.J., & Ge, J. 1996, *ApJ*, 456, L13
- Fraternali, F., van Moorsel, G., Sancisi, R., & Oosterloo, T. 2002, *AJ*, 123, 312
- Gruenwald, R., & Viegas, S.M. 1993, *ApJ*, 415, 534
- Guillemin, P., & Bergeron, J. 1997, *A&A*, 328, 499
- Holmberg, E. 1975, in A. Sandage & J. Kristian (eds.), *Stars and Stellar Systems: Galaxies and the Universe*, vol. 9, p. 123
- Kacprzak, G.G., Churchill, C.W., & Steidel, C.C. 2005, in P.R. Williams, C. Shu, & B. Ménard (eds.), *Probing Galaxies through Quasar Absorption Lines*, (IAU), vol. 199, *this volume*
- Kobayashi, N., Terada, H., Goto, M., & Tokunaga, A. 2002, *ApJ*, 569, 676
- Lanzetta, K.M., Turnshek, D.A., & Wolfe, A.M. 1987, *ApJ*, 322, 739
- Lanzetta, K.M., & Bowen, D. 1990, *ApJ*, 357, 321
- Lanzetta, K.M., & Bowen, D. 1992, *ApJ*, 391, 48
- Le Brun, V., Bergeron, J., Boissé, P., & Christian, C. 1993, *A&A*, 279, 33
- Le Brun, V., Bergeron, J., Boisse, P., & Deharveng, J. M. 2001, *A&A*, 321, 733
- Lin, W-P., & Zou, Z-L. 2001, *ChJAA*, 1, 21
- Masiero, J.R., Charlton, J.C., Ding, J., Churchill, C.W., & Kacprzak, G.G. 2005, *ApJ*, in press (astro-ph/0501139)
- Malhotra, S. 1997, *ApJ*, 488, L101
- Mo, H.J., & Miralda-Escudé, J. 1996, *ApJ*, 469, 589
- Ménard, B. *et al.*, 2005, in P.R. Williams, C. Shu, & B. Ménard (eds.), *Probing Galaxies through Quasar Absorption Lines*, (IAU), vol. 199, *this volume*
- Nestor, D.B., Turnshek, D.A., & Rao, S.M. 2005, *ApJ*, in press (astro-ph/0410493)
- Petitjean, P., & Bergeron, J. 1990, *A&A*, 231, 309
- Phillipps, S., Disney, M.J., & Davies, J.I. 1993, *MNRAS*, 403, L55
- Prochter, G.E., Prochaska, J.X., & Burles, S. 2005, *ApJ*, submitted (astro-ph/0411776)
- Rigby, J.R., Charlton, J.C., & Churchill, C.W. 2002, *ApJ*, 565, 743
- Rand, R. 2000, *ApJ*, 537, 13
- Rao, S.M., Nestor, D.B., Turnshek, D.A., Lane, W.M., Monier, E.M., & Bergeron, J. 2003, *ApJ*, 595, 94
- Rao, S.M., & Turnshek, D.A. 2000, *ApJS*, 130, 1
- Sancisi, R., Fraternali, F., Oosterloo, T., & van Moorsel, G. 2001 in J.E. Hibbard, M.R. Rupen, & J.H. van Gorkom, *The HI Halos of Spiral Galaxies*, (PASP), vol. 240, p. 241
- Sargent, W.L.W., Steidel, C.C., & Boksenberg, A. 1988a, *ApJS*, 68, 539
- Sargent, W.L.W., Steidel, C.C., & Boksenberg, A. 1988b, *ApJ*, 334, 22
- Simard, L., Willmer, C.N.A., Vogt, N., Sarajedini, V. L., Phillips, A.C., Weiner, D., Koo, D.C., Myungshin, I., Illingworth, G.D., & Faber, S.M. 2002, *ApJS*, 142, 1
- Srianand, R., & Khare, P. 1993, *ApJ*, 413, 486
- Steidel, C.C. 1993, in S.R. Majewski (ed.), *Galaxy Evolution: The Milky Way Perspective*, (PASP), vol. 49, p. 227
- Steidel, C.C. 1995, in G. Meylan (ed.), *ESO Workshop on Quasar Absorption Lines*, (Springer-Verlag), p. 139
- Steidel, C. C. 1998, in D. Zaritsky (ed.), *Galactic Halos: A UC Santa Cruz Workshop*, (PASP), vol. 136, p. 167
- Steidel, C.C., Dickinson, M., Meyer, D.M., Adelberger, K.L., & Sembach, K.R. 1997, *ApJ*, 480, 568
- Steidel, C.C., Dickinson, M., & Persson, S.E. 1994, *ApJ*, L75
- Steidel, C.C., Kollmeier, J.A., Shapley, A.E., Churchill, C.W., Dickinson, M., & Pettini, M. 2002, *ApJ*, 570, 526
- Steidel, C.C., & Sargent, W.L.W. 1992, *ApJS*, 80, 1
- Tytler, D., Boksenberg, A., Sargent, W.L.W., Young, P., & Kunth, D. 1987, *ApJS*, 64, 667
- Yanny, B. 1990, *ApJ*, 351, 396
- Vogt, S.S., *et al.* 1994, in D.L. Crawford & E.R. Craine, *Instrumentation in Astronomy VIII*, (SPIE), vol. 2198, p. 362
- Zonak, S.G., Charlton, J.C., Ding, J., & Churchill, C.W. 2004, *ApJ*, 606, 196